

A Study on the Orientation Effects in Polyethylene in the Light of Crystalline Texture

Part 4 *Truly Single Texture on Unidirectional Rolling*

J. J. POINT

Faculte Polytechnique, Mons, Belgium

G. A. HOMÉS

Faculte des Sciences, Mons, Belgium

D. GEZOVICH, A. KELLER*

Polymer Division, Case Western Reserve University, Cleveland, Ohio, USA

Received 24 May 1969

As a continuation of previous works aimed at obtaining macroscopic specimens of polyethylene with a simple texture, samples were prepared by unidirectional rolling (without previous drawing) followed by heat-relaxation. This resulted in a macroscopic lamination consisting of two transparent outer zones and a turbid zone in the interior. It was confirmed by full pole figure analysis, both at wide angles involving three reflections and at low angles, that the two transparent edge zones were truly single-textured as regards both the subcell and the superperiod, the orientation at the two edges being in mirror relation. The middle zone corresponded partly to a superposition of the structure at the two edges, but contained also additional complicating features. The new findings support several of the basic assumptions made in the previous papers of the series based on less complete evidence. Further, they provide the best characterised and most uniquely defined textures known in a polycrystalline polymer so far, in a form suitable for further macroscopic examination. Also the present findings should be relevant to the interpretation of the crystal morphology of oriented polymers in general and to the understanding of the rolling process in particular.

1. Introduction

It is self-evident that exploration of both structure and properties of crystalline polymers calls for samples which are as uniquely defined as possible from the crystallographic standpoint. Of course, individual single crystals would be desirable. Such, however, have not yet been obtained in the form of macroscopic entities and in any case polymers as used for technological purposes are polycrystalline aggregates containing some disordered material. The course usually taken is to convert the initially random aggregate into an oriented form where one or

more of the crystal axes in the different crystallites are aligned with respect to macroscopically identifiable directions in the sample.

The oriented state most readily realised is obtained by drawing, which leads to cylindrical (fibre) symmetry with one crystal axis – the one coincident with the chain direction – along the fibre, i.e. the draw direction, the others being randomly arranged around it. This latter randomness can be further reduced by rolling. This as a rule leads to a double texture, the two components being in twin relation [1-4]. In the case of polyethylene a further reduction to an

*Permanent address: H. H. Wills Physics Laboratory, University of Bristol, Tyndall Avenue, Bristol, UK. The exploratory work was carried out by J. J. Point, at this address, during a temporary stay.

approximately single texture can be achieved by slightly annealing this double texture [1, 2, 5]. In this case the c -(the chain) direction is along the draw and rolling direction (Y , fig. 1). (In fact there is usually a slight inclination in both senses about Y in the XY plane, which means that the structure is slightly doubled. Past references to a single texture, while adequate for the purposes quoted [3, 6, 7] thus contained simplifications.) The a -axes were along the normal to the rolling plane (X) (with the same simplification as for the c -axes) while b was lying in the film plane perpendicular to X and Y (Z direction, see fig. 1). This b alignment was always exact.

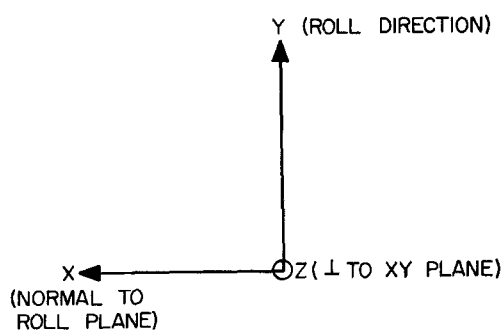


Figure 1 Definition of axes.

Nevertheless such structures were approximately single only as regards the orientation of the unit cell. Discrete X-ray reflections at low angles are also present, indicating a superstructure on the 100 Å scale, usually associated with a more or less regular stacking of lamellar crystallites. The above-quoted single textures give a so called "four-point" diagram at low angles with the beam along Z (i.e. b) the corresponding pole (n pole) being in the ac plane at an angle of 45° with respect to c . In terms of the lamellar model this was interpreted as a double lamellar texture [3, 8, 9]. Accordingly the lamellar interfaces are $\{h0l\}$ type, $\{301\}$ in particular, but present in two sets, (301) and $(\bar{3}01)$, corresponding to two equal but opposite inclinations with respect to the c -axes. It follows therefore that samples with closely single orientations as regards the unit cell are still strongly double textured as regards the superstructure.

The main purpose of the present paper is the reporting of the preparation and characterisation of samples which are truly single textured also on the level of the superstructure. Of the extensive material available, only a selection will be

quoted here so as to make the point just stated. More comprehensive publications will follow.

2. Experimental Methods

2.1. Preparation of Samples

The effects in question appeared most clearly when films of unoriented low density polyethylenes were rolled only (without preceding drawing, in direct continuation of earlier work by one of us [5]) the sample being passed always along the *same* direction through the rollers. Films initially 5 mm thick were reduced to about 2 mm thickness in the process. The samples were then heat-relaxed between 90 and 110° C. The systematic variations with relaxation temperature will be reported elsewhere [10]. Here it will merely be stated that as a result of annealing, an inhomogeneous structure developed even on inspection of the sample when viewed along Z . As seen from fig. 2, the sample is stratified

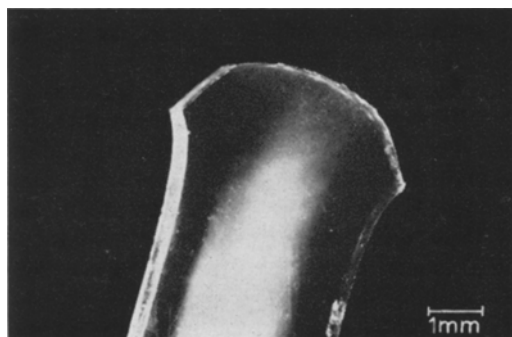


Figure 2 Photograph of a section in the XY plane of a sample of low density polyethylene rolled unidirectionally and annealed at 100° C as seen along Z . Y vertical, X horizontal (approximately).

parallel to the roll direction into three zones. The two zones along the edges are transparent and the central zone is turbid. The sample thickens along X with increasing annealing temperature with an accompanying increase in width, both absolute *and* relative, of the transparent zones. There are also corresponding changes in the contours at the sample end (fig. 2). These latter effects are due to unequal contraction of the zones, an effect to be elaborated elsewhere [10].

2.2. X-ray Examination Methods

The three zones were examined by both wide- and low-angle X-ray diffraction.

2.2.1. Wide-Angle X-ray Diffraction

In addition to stationary photographs taken in different sample orientations – the only method adopted in earlier work – the full pole figures were also recorded in some selected specimens. The samples to be examined in this way were dissected into the three macroscopically visible zones each of which was then mounted as an isolated strip on the goniometer. A Picker single crystal analyser combined with a computerised counting and plotting system was used for the pole figure determinations in a conventional way. Three poles, 020, 200, and 110, were mapped, over a full hemisphere centred on X in each case.

2.2.2. Low-Angle X-ray Diffraction

Here again both stationary photographs and full pole figures were recorded. Franks and Rigaku Denki cameras were used in different stages of the work with point collimation. The stationary photographs were taken along the lines adopted in earlier works; the recording of the pole figures, however, is to our knowledge the first of its kind in the low-angle region, consequently the technique merits some comments.

The Rigaku-Denki low-angle diffractometer was used with 0.3 mm point collimation. The set-up was similar to that described by Cullity [11]. The sample was first mounted with Z along the beam direction and the diffractometer was set at the peak maximum in 2θ (which in the present sample to be reported here was 0.80° , corresponding to a Bragg spacing of 110 Å). Then the sample was rotated manually around Z , taking readings at every 10° , over the full range of 360° . The sample was then rotated through 10° around Y (originally mounted so as to be along the rotation axis of the goniometer) and readings were again taken for a full 360° rotation around Z . This process was continued for successive 10° rotations around Y until the ring shaped sample-holder began to obstruct the beam as it approached an edge-on position with respect to it. At this stage the sample was remounted so that X was normal to the plane of the sample-holder ring and hence could be brought conveniently parallel to the beam. Now the previous procedure was repeated, namely rotation around X in successive sample settings around Y . This ensures the full mapping of a hemisphere centred either on Z or X , including some areas mapped twice to serve as a check. In regions of high intensity or where intensity was changing rapidly, data were taken every 5° in

order to ascertain the size and shape of the strong poles.

As will be seen, the pole figures confirmed the previous assertions based on stationary photographs only, that the maxima of the n poles lie in the XY plane. This means that stationary photographs with the beam along Z should provide most of the information relevant for the present purpose, i.e. they should suffice to define the position of the maxima within the XY plane. In addition they can give the intensity distribution over different θ values at least within (or close to) the XY plane and thus reveal layer lines and streaks which are not apparent from the pole figures appropriate to the chosen 2θ value. (Pole figures for a continuous range of 2θ values would contain this information and much more; this, however, was not carried out.) Stationary photographs also served an additional purpose: with the beam along Z , a detailed point to point scan was made across the sample along X , exploring the extreme edges and the transition regions between the zones in this one, and as it happened significant, projection.

3. Results

The data to be reported here were mostly obtained on one particular unidirectionally rolled sample annealed at 90°C ; less complete data on other samples are all essentially in line with those to be given here. Fig. 3 is a sketch of a sample viewed along Z to serve as a reference.

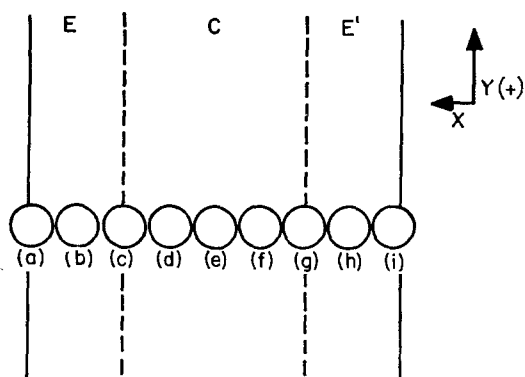


Figure 3 Sketch of sample seen along Z with reference to diffraction patterns. The encircled points represent the localities from which the low-angle diffraction patterns in fig. 10 were taken denoted by the appropriate letters. This latter assignment is schematised, as fig. 3 is not strictly to scale (amongst others zones E and E' were not identically wide in the actual specimen). Directions correspond to those in figs. 4–9 in their present mounting.

E , E' and C are the two transparent edges and the turbid central zone respectively.

3.1. Establishment of Single Texture in Zone E

Figs. 4a, b, c, give the pole figures of zone E for the 020, 200, and 110 reflections respectively.

As is apparent there is one prominent maximum for the 020 and 200 poles and two for the 110 poles, pairs of equivalent poles, i.e. those related by centre of symmetry, being counted as one. In addition there are some weak maxima just at the perception level of our recording sensitivity. Concentrating on the dominant strong maxima

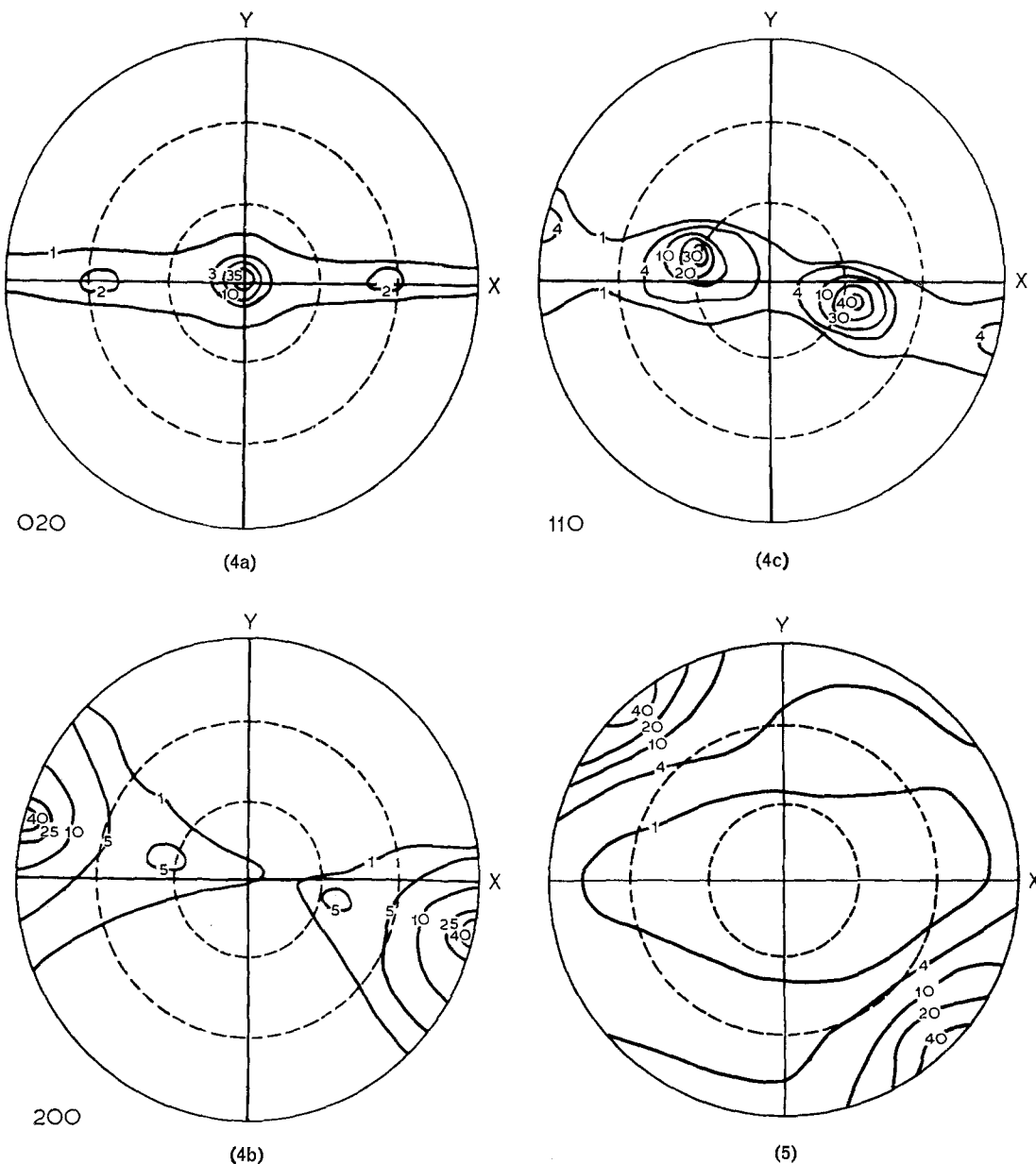


Figure 4 Pole figures for three wide-angle X-ray reflections corresponding to zone E. A full hemisphere centred on X was actually mapped. It was redrawn as centred on Z by utilising the centro-symmetric nature of the full pole figure. (a) 020, (b) 200, (c) 110.

Figure 5 Low-angle X-ray reflection pole figures for zone E (for particulars see text).

first, it will be seen that 020 is exactly along Z and 200 is at 90° to it in the XY plane at 14° to X . These being the only strong pole concentrations, it appears justified to associate them with the *same* crystals giving rise to both. It will be apparent that this assignment defines a single-orientation of the unit cell. This assignment is fully supported by the two strong 110 maxima which, as can be read off directly from fig. 4c, correspond to the 110 and $1\bar{1}0$ poles in the single texture already defined above by the 020 and 200 poles. Although 001 poles were not determined directly (the reflections are very weak) the orientation of c can now be uniquely assigned: the maximum of c is in the XY plane inclined through 14° from Y pointing *towards* the sample interior when looking along the rolling direction (+ Y is upwards in figs. 4 to 10).

The main features of the very weak secondary maxima are the single 110 peak close to X but slightly inclined in the XY plane and the two 200 and 020 peaks close to the ZX plane. On the plausible assumption that there is a further pair of 110 maxima, but coincident with the strong maxima previously associated with the dominant single orientation, the weak peaks would correspond to a pair of single textures in (310) and ($3\bar{1}0$) (or the closely similar (110) and ($1\bar{1}0$)) twin relation to the dominant single texture. These are in fact the twin modes expected *a priori* [1, 12, 13] and are known to be responsible for textures produced by rolling or compressing previously drawn material [1, 2, 8, 12, 13] on removal of pressure. These are the textures which are converted into a single texture by heat-treatment. Accordingly, the presently observed weak maxima should be remainders of the original twinned texture due to rolling which had not been fully removed by the annealing. However, as is apparent, these twinned textures represent only a minute fraction of the total amount of material and would have remained undetected by the texture examination methods applied in the past. We may state therefore that on the existing standards of polymer texture studies a single orientation of the unit cell with unusually sharp definition has been realised.

Fig. 5 is the pole figure for the maximum of the low angle reflection in an orientation corresponding to the pole figures of fig. 4. In the series of stationary photographs with beam along Z (fig. 10), photographs 10a, b and perhaps also

fully or partially 10c, correspond to zone E (see fig. 3) which was used as a whole for the pole figure determinations*. As can be seen there is one pair of maxima, the corresponding n poles being at 40° to Y in the direction given directly by the pole figure and photographs. It follows that we now have a single texture also on the superstructure scale, uniquely specified both with respect to the macroscopic sample dimension and the orientation of the unit cell.

3.2. The Relation Between the Two Edge Zones

The next question concerns the nature of the discontinuities giving rise to the zones. Figs. 6a-c are the wide-angle pole figures of zone E', i.e. the transparent zone along the opposite sample edge. Even if the pole distributions are somewhat less symmetrical (this is likely to be due to less perfect sample alignment in the goniometer, a difficult procedure in view of the fact that the cutting may not be exactly in the XY plane) the pattern is similar to that given by zone E. Thus it is again attributable to a dominant single texture with b along Z and a in the XY plane at 14° to X . However, in this case the inclination of a is in a direction which is opposite to that in E which makes the c -axis tilted again towards the sample interior when looking along the rolling direction.

The low-angle pole figure for zone E' is shown in fig. 7, and the corresponding stationary photographs in figs. 10g and h (fig. 10i will be commented on separately later). As seen there is again one pair of maxima. This is again in the XY plane at 40° to Y but on the opposite side of Y as compared with zone E. (The two-point patterns in figs. 10g and h are consistent with the pole figures, given by the zone as a whole, but there is a small reduction of the angle $n^\wedge Y$ within the zone towards the sample interior, i.e. from fig. 10h to fig. 10g). It follows that there is an identical relationship between the respective superstructures and unit cell orientations in the two transparent zones.

It is interesting to note that the double textures studied previously [3, 8, 9] were of the type produced by the superposition of the two transparent zones both as regards unit cell and superstructure. This is very satisfactory in view of the fact that the earlier assignment was arrived at without a full pole figure analysis, hence was not necessarily unique. The present results

*It appears that there is also a further reflection pair at the same azimuth closer to the centre (1st order?). Neither this point nor the whole question of the actual value of the interplanar spacing will feature in the present paper.

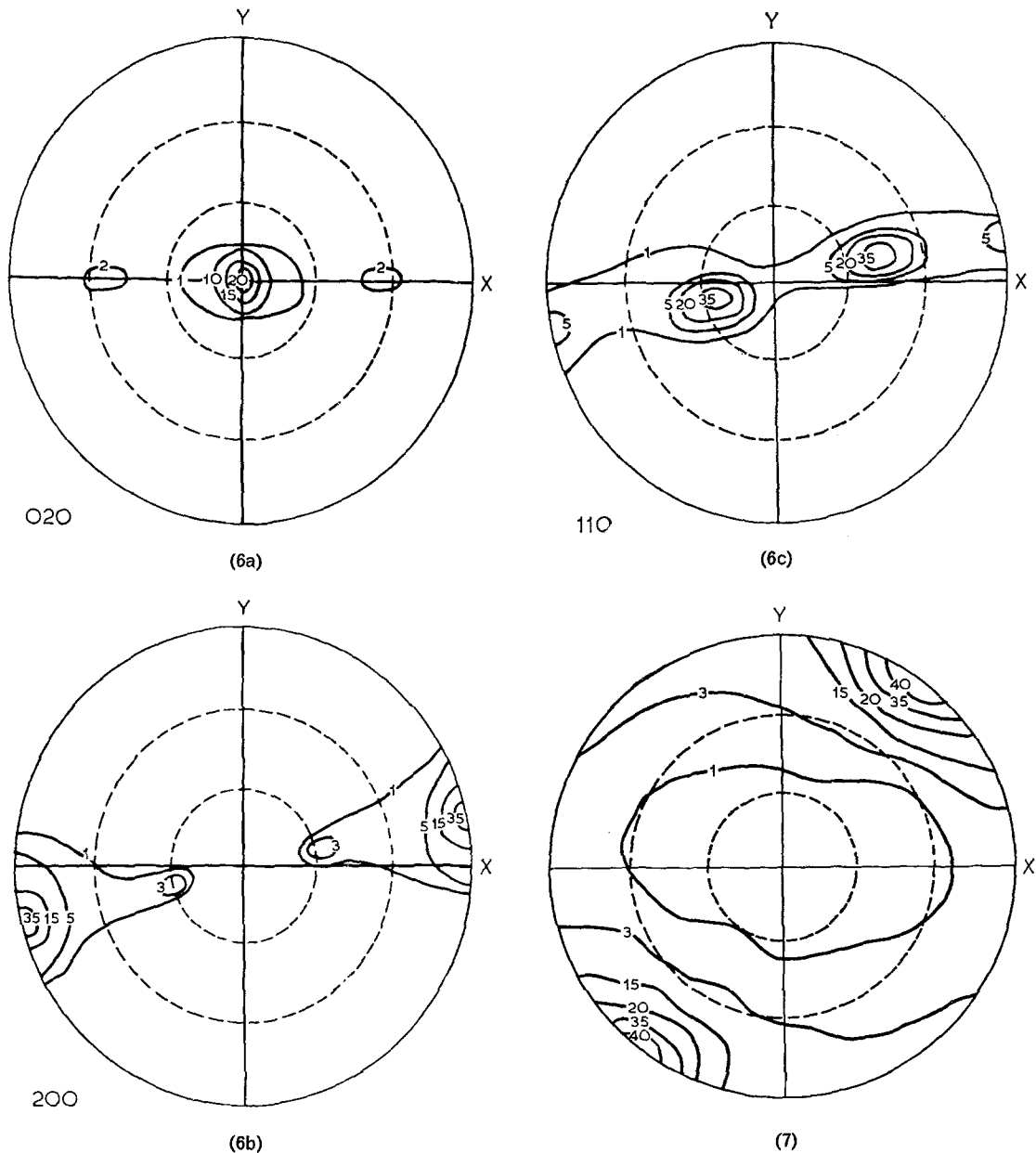


Figure 6 Pole figures for three wide-angle X-ray reflections corresponding to zone E'. Particulars as in caption to fig. 4. (a) 020, (b) 200, (c) 110.

Figure 7 Low-angle X-ray reflection pole figure for zone E' (for particulars see text).

therefore provide added justification to the earlier conclusions drawn from selected stationary diffraction patterns both in the wide- and low-angle regions.

Fig. 11 shows a superposition of two low-angle patterns from the two transparent zones of the same specimen (this particular sample was annealed at 97°C where the c inclination is

larger). This is the type of pattern obtained previously on the double textured samples, the principal feature being the characteristic inclinations of the lobes in the four-point diagram. Previously this was interpreted in terms of streaks associated with each component of the double texture [2, 9], an interpretation now receiving further support.

3.3. The Central Zone (C of Fig. 3)

The pole figure for 020 again reveals a single maximum along Z (fig. 8a). Also there are two 200 maxima in the XY sample plane at $\pm 14^\circ$ from X (fig. 8b). However, there is also an additional broad 200 maximum around Z. There are two 110 maxima; they are broad and are centred on the XZ plane (fig. 8c). In so far as the

200 poles in the XY plane are associated with the crystals, giving rise to the 020 maxima on Z, we can say that zone C contains the textures in zones E and E' in combination, which is a reasonable expectation. The 200 maximum, centred on Z however, has no simple interpretation. The associated 020 poles cannot lie on Z neither is another 020 maximum seen. Con-

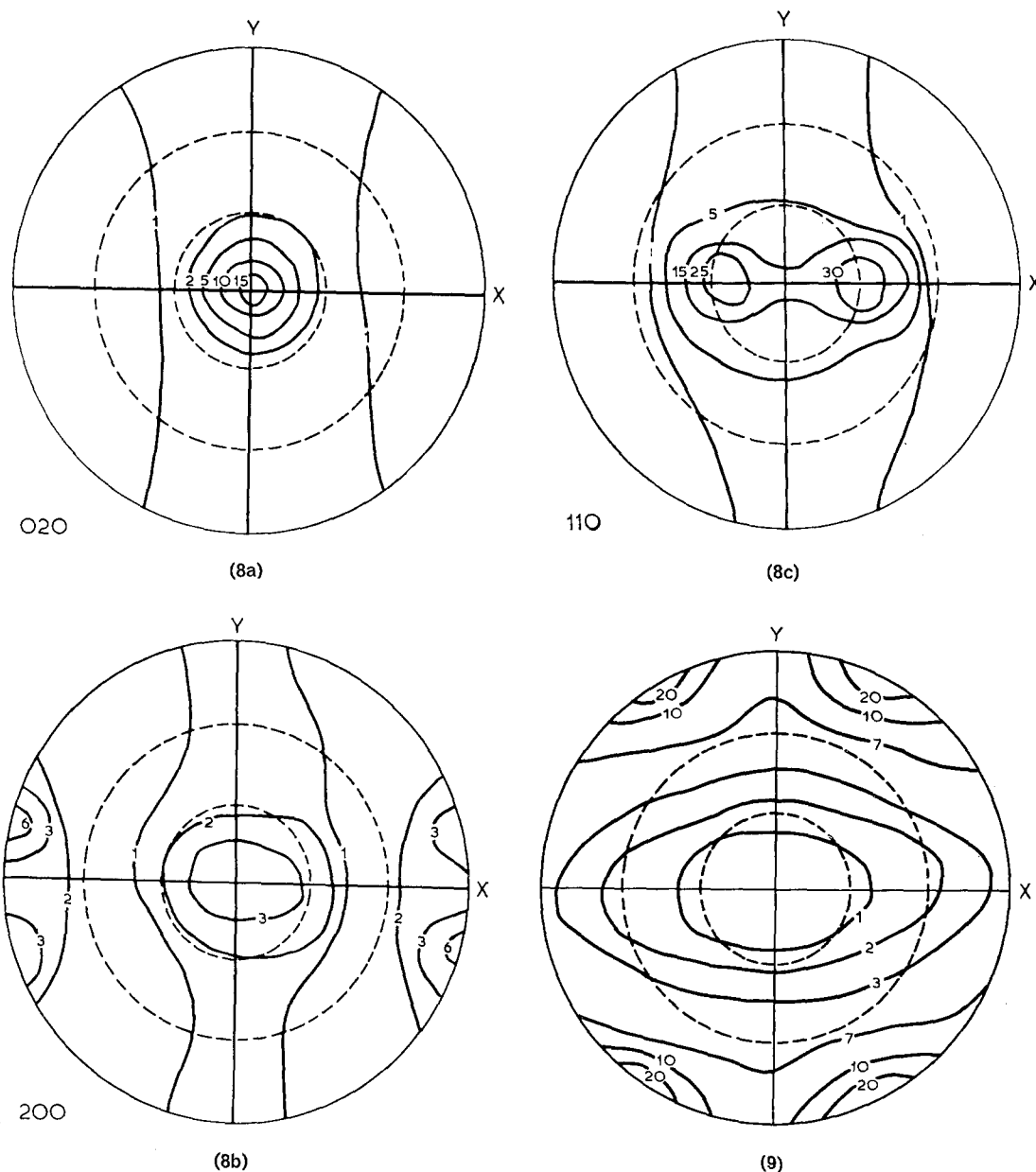


Figure 8 Pole figures for three wide-angle X-ray reflections corresponding to zone C. Particulars as in caption to fig. 4. (a) 020, (b) 200, (c) 110.

Figure 9 Low-angle X-ray reflection pole figures for zone C (for particulars see text).

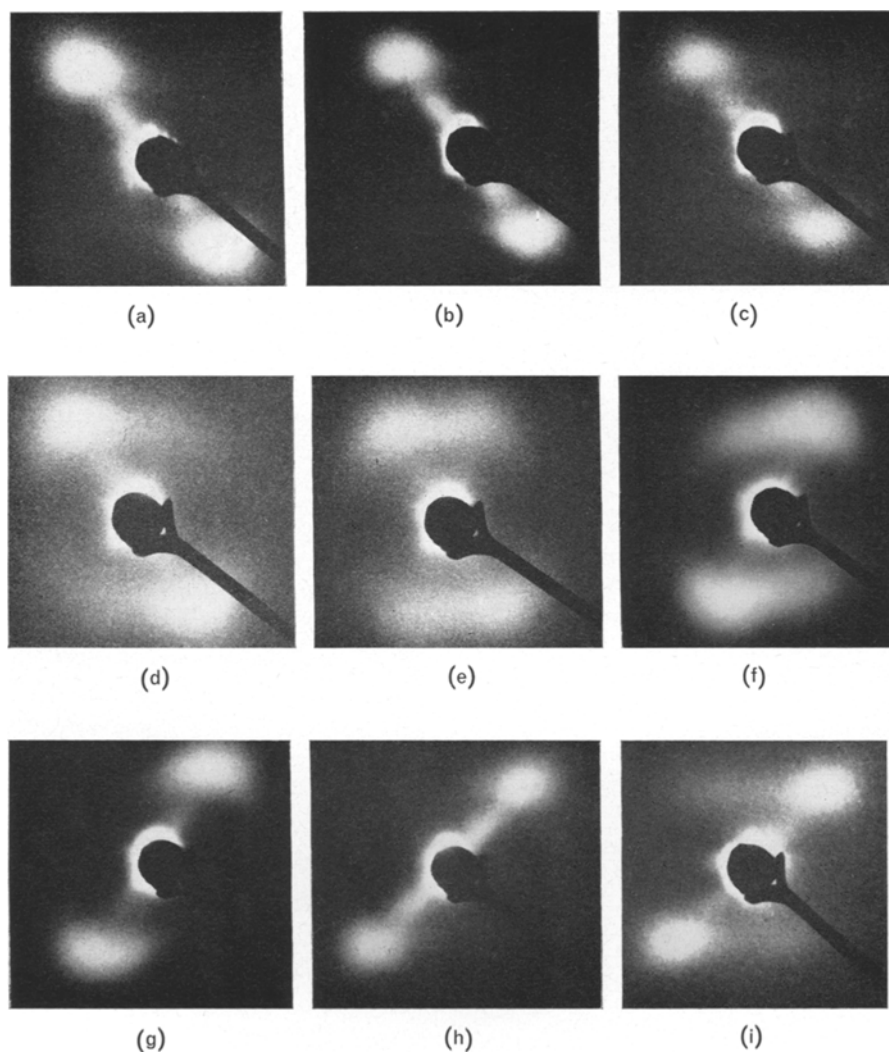


Figure 10 Series of low-angle diffraction patterns with beam along Z , and Y vertical. The lettering corresponds to the locations marked in fig. 3.

sequently, crystals contributing to the 200 pole in question must display a broad distribution in b -axes, such as would not become distinct enough from the background with our sensitivity of detection. The position of the 110 poles is broadly consistent with the 020 poles being on Z ; however, a small split about the ZX plane would be expected, in order to be consistent with the 200 maxima in the XY plane. This split is not resolved; undoubtedly the crystals in the unaccounted orientation referred to above obscure the issue. (Incidentally, this example illustrates the difficulty of pole figure interpretations in the presence of more than one orientation, especially if diffusely defined.)

Low-angle diffraction by zone C yielded the pole figure of fig. 9. It possesses maxima in the XY plane at 20 to 26° both sides of Y . The corresponding stationary photograph with the beam along Z is shown by fig. 10e, which is a four-point diagram as is to be expected from the pole figure.

Here again, the maxima are only at (20 to 26°) with respect to Y as opposed to around 40° along the sample edges, and also the reflections as revealed by the photograph curve slightly rather than follow straight layer lines as they do in the edge zones.

As is apparent, the texture in the central zone can be regarded as a superposition of those at the

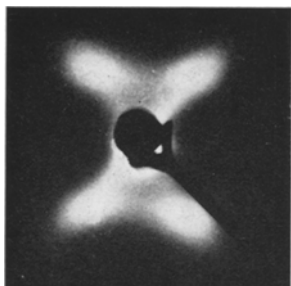


Figure 11 Superposition of two low-angle X-ray diffraction patterns taken of E and E' zones of a unidirectionally rolled sample annealed at 97° C. The beam is along Z.

two sample edges only in its broadest outlines. In the wide-angle patterns it certainly contains a component corresponding to such a superposition but it also displays additional features. In the low-angle patterns the symmetry indicates such a composite structure but there are differences in the inclination and the shape of the reflections. In this latter respect it certainly differs from the previously investigated drawn and rolled structures (there is no complete comparison as pole figures have not been recorded in the drawn and rolled structures) which appear to correspond to the sum of the two edge zones of the rolled only material, as mentioned in the preceding chapter.

3.4. Transition Regions

With the small beam size in the low-angle experiments, further details could be examined. The stationary photographs of figs. 10c, d, f, and g correspond to transition stages between edge and centre at the two sample sides (see fig. 3). There are four maxima asymmetric both as regards intensity and position (figs. 10c, d). The more intense pair corresponds approximately to the one visible in isolation further towards the sample edge at the same sample side. The weaker pair is at a slightly smaller diffraction angle on the opposite side of Y but closer to it. Thus, the four maxima define a skew rectangle in mirror relation on the two sides of the sample. The reflections are slightly curved and it appears that they could result from the superposition of an edge and a centre pattern such as for instance figs 10a and e.

So far, the pattern in fig. 10i has received no specific comment. This is also an asymmetric four point pattern, but distinct from the ones just described. In the first place it does not come from the transition area between transparent and

turbid zones but from the extreme sample edge, thus reversing the trend from double to single texture towards the edge. Secondly, the character of the pattern is different. The maxima are now along well defined layer lines. While the corresponding pattern could not be obtained along the opposite edge of the particular sample analysed here in detail, patterns of this type were frequently observed in other specimens, sometimes also from both sample edges when the patterns were in mirror relation. Fig. 12 shows an example with a more distinct weaker pair.

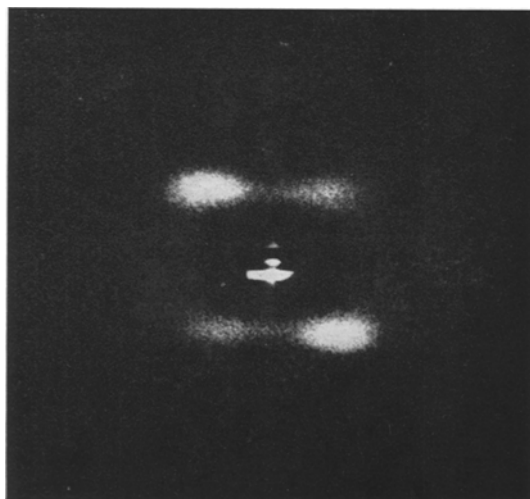


Figure 12 Low-angle X-ray pattern taken of the extreme edge of a unidirectionally rolled sample.

4. Interpretation

The significance of achieving simple crystal textures in polymer studies has already been emphasised. We see that samples have now been obtained which come as close to possessing a single texture, both as regards crystal lattice and superstructure, as one can expect to achieve in a polycrystalline polymer. The homogeneity of the texture on the scale of light waves is also indicated by the transparency of the appropriate sample portions. The samples can be obtained in sufficient size for making them suitable for most physical tests.

So far, the outcome of the present studies is straightforward. However, enquiries about the nature of the superstructural elements, about the particulars and the origin of the zoning across the sample raises some further issues to be touched upon only briefly here.

As is familiar, low-angle X-ray maxima are usually associated with a lamellar structure. In the earlier work this has led to the formulation of a model of lamellar slip processes which helped to account for structural effects observed in the course of heat-induced shrinkage, and externally induced extensions and compressions [3, 9]. It also proved to be a fruitful concept for the interpretation of mechanical anisotropy (interlamellar shear) in the Hookeian elastic range [6, 7]. Adoption of the lamellar picture for the dominant texture for the edge zones of the present sample implies a single, oblique lamellar orientation with respect to the rolling direction with the chains inclined to the lamellar surface. As before, this inclination is predominantly in the *ac* plane leading to $\{h0l\}$ basal surfaces. In previous work this angle was close to 45° (corresponding to $\{301\}$) remaining constant over a significant range of crystal orientations induced by heat shrinkage, redrawing and compression [3, 9]. In the present single texture sample portions this angle would be 54° , arrived at from the combination of the appropriate wide- and low-angle pole figures, which would correspond close to a $\{401\}$ basal surface. This is certainly more oblique than anything found before. Inspection of the low-angle photographs in fig. 10, however, shows that the angle $n^\wedge Y$ decreases across the transparent zone from edge to centre (it is 40° in fig. 10h and 28° in fig. 10g). Consequently, dependent on which portion was responsible for the pole figure at both wide- and low-angles, the true $c^\wedge n$ angle may possibly be smaller than 54° . For a more accurate assessment, however, a finer subdivision for the correlation of wide- and low-angle textures would be required.

On the basis of the lamellar picture, there should be two sets of lamellae of opposed inclination within zone C and an appropriate mixture of the two, corresponding to the intensity ratios of the maxima, within the transition ranges. However, the $n^\wedge Y$ angle is smaller in zone C, which implies a smaller angle $c^\wedge n$, hence less oblique lamellae in the central compared with the lateral zones. The non-uniqueness of the lamellar obliquity has already been implied in earlier work. In the first place, a change from $\{301\}$ to the less oblique $\{201\}$ has been inferred at a particular stage of heat-relaxation [3]. Secondly the streaking of the low-angle maxima was attributed to the simultaneous presence of a range of lamellar obliquities rather than to a spread of the interference function due

to small crystals (very narrow stack of lamellae) [3, 9]. The existence of different obliquities, even within the same macroscopic sample, has now been demonstrated. This provides further basis for the contention that the streaking could arise through a superposition of diffraction effects due to a range of lamellar obliquities. The further implication of this is that the lamellae are sufficiently extended laterally to give rise to Bragg type diffraction maxima, where packets corresponding to each obliquity contribute to the intensity along the appropriate portion of the layer line streak.

Of course the uniqueness of the interpretation of diffraction effects can always be scrutinised, particularly when so little information is available as in the low-angle patterns. The asymmetric four-point patterns, as in figs. 10i and 12 in particular, could lend themselves to alternative interpretations. In this context a definitive experimental statement is still lacking. Namely, are both low-angle maxima associated with the same *c* orientation or are there two corresponding lattice orientations? This question is still unanswered, since at present we have no pole figures corresponding to sample portions giving rise exclusively to patterns like those in figs. 12 and 10i. A single *c* orientation which appears the most plausible from the evidence available so far would imply two sets of lamellae with identical chain orientation but of opposed and slightly different basal plane inclinations, the one with the larger obliquity being the dominant species. In this case the layer line streak should be normal to the chain direction, a feature which underlies the interpretation of some of the earlier work on the double texture [3]. This emerges also from much of the new material [10] although, as already stated, a finer subdivision of the sample as regards pole figure mapping both at wide- and low-angle examination would be required for a definitive statement on this point.

The asymmetric four-point patterns, as in figs. 10i and 12, raise an alternative interpretive possibility. One could regard the four maxima as defining a two-dimensional superlattice. We refrain from specifying such a possible lattice in structural terms at this juncture; this will be done elsewhere. Here it should suffice to state that a plausible structural model can be thought of which is in accord with observations on the dimensional changes of the edge zones on heat-induced shrinkage (to be published separately [10]).

One of the most important further questions concerns the relation of the newly observed textures, the single texture in particular, to the deformation process. Rolling is a composite deformation process with severe shear involved. In order to produce the single textures in isolation in a controlled manner it would be necessary to know the stress system giving rise to it. Conversely rolling itself is an important deformation mode in polymer fabrication. Understanding of the genesis of the presently reported textures would lead to a better appreciation of the rolling process. All this would require extensive further investigations, some of which are in progress. A general point which is implicit in the present result is that unidirectional rolling, as opposed to straightforward drawing, produces (in combination with appropriate heat-treatment) a "polar" texture: the directions parallel and antiparallel to the roll direction (+ Y and - Y in fig. 3) are non-equivalent with respect to the resulting texture.

Acknowledgement

D.G. and A.K. would like to thank Professor P. H. Geil for his stimulating interest and Mr A. Burmester for his help in obtaining the small angle pole figures. They are greatly indebted to Professor M. Sundaralingham for access to his X-ray facilities used in part of the work. A.K. wishes to thank Professor E. Baer for hospitality

and support at Case Western Reserve University while on leave of absence from the University of Bristol.

References

1. F. C. FRANK, A. KELLER, and A. O'CONNOR, *Phil. Mag.* **3** (1958) 64.
2. I. L. HAY and A. KELLER, *J. Materials Sci.* **1** (1966) 41 (part 1 of series).
3. *Idem, ibid* **2** (1967) 538 (Part 2 of series).
4. C. W. BUNN and E. V. GARNER, *Proc. Roy. Soc.* **A189** (1947) 39.
5. J. J. POINT, *Memoires et Publications de la Societe des Science des Arts et des Lettres du Hainaut* **71** (1958) 65.
6. V. B. GUPTA and I. M. WARD, *J. Macromol. Sci.* **B2** **1** (1968) 89.
7. Z. H. STACHURSKI and I. M. WARD, *J. Polymer Sci.* **A2** **6** (1968) 1817.
8. T. SETO and Y. TAJIMA, *Jap. J. Appl. Phys.* **5** (1966) 534.
9. A. COWKING, J. G. RIDER, I. L. HAY, and A. KELLER, *J. Materials Sci.* **3** (1968) 429 (part 3 of series).
10. J. J. POINT and A. KELLER (to be published).
11. B. D. CULLITY, "Elements of X-ray Diffraction" (Addison-Wesley, 1959) p. 285.
12. I. L. HAY and A. KELLER, IUPAC Symposium, Toronto (1969). Preprint **A6** **8**, *J. Polymer Sci.* in the press.
13. T. SETO, T. HARA, and K. TANAKA, *Jap. J. Appl. Phys.* **7** (1968) 31.